Progress In Electromagnetics Research, PIER 66, 179–190, 2006

CRANKLED S-RING RESONATOR WITH SMALL ELECTRICAL SIZE

H. Chen, L. Ran, B.-I. Wu, J. A. Kong and T. M. Grzegorczyk

The Electromagnetics Academy at Zhejiang University
Zhejiang University
Hangzhou 310058, P. R. China
and
Research Laboratory of Electronics
Massachusetts Institute of Technology
Cambridge, MA 02139

Abstract—Metamaterials with small electrical size are more feasible to be described by the macroscopic parameters and treated as an effective homogenous media. By using geometric optimization, we experimentally realize a metamaterial composed of crankled S-ring resonator, whose electrical size is 2.5 times smaller than the conventional S-ring resonator. The overall effective capacitance of the unit structure is greatly increased when viewed from an equivalent circuit model point of view, so the resonant frequency is decreased, and the metamaterial works at a much longer wavelength regime. In addition, we summarize two kinds of other methods that could be used to reduce the electrical size of the structures. Experimental and simulation results are presented, showing the effectiveness of these methods in the metamaterial homogenization.

1. INTRODUCTION

Left-handed metamaterials (LHMs) have drawn particular attention [1–11] due to the property of negative refractive index, which is associated with a simultaneously negative permittivity ϵ and negative permeability μ, and results in many unusually phenomena such as the reversal of Snell's law, the Doppler effect, and Cerenkov radiation [1]. Left-handed metamaterials are not available in nature but has been artificially realized and verified based on the split-ring resonator (SRR) and thin wires [2–7]. Recently, other metamaterial structures, such as

the symmetrical ring resonator [2, 12], Ω-like structure [13], S-shaped resonators [14, 15], etc, have been reported and shown to exhibit left-handed properties. Some photonic crystals reported have also been shown to support backward wave and exhibit negative refraction [16]. Different from photonic crystals, where the lattice constant is typically of the order of half the operating wavelength, LHMs operates in the long-wavelength regime, where the lattice constant is much smaller than the operating wavelength. In this case, the structural units in the metamaterials are analogous to the atoms or molecules in a homogenous media, such as air, water, etc. Hence the metamaterial structures exhibit a macroscopic behavior and can be treated as a homogenous material described by an effective permittivity and permeability [17, 18]. In the metamaterial structures reported so far, the structural unit size is often in the range of $\lambda/5 \sim \lambda/15$, where λ is the operating wavelength. It has been reported that if the structural unit size approaches $\lambda/4$, some parasitic diffraction effects can be included, so decreasing the unit size of left-handed metamaterials can mitigate these parasitic effects [19]. However, to achieve a homogenous left-handed material is very difficult to realize in practice. There are usually three methods, as summarized here, to decrease the electrical size of the metamaterials. The first one is to optimize the parameters of the ring. For example, in the SRR structure, by changing the geometrical parameters like the gap between the rings, and the metal width, the ring can be optimized to have a small electrical size. This method has been widely investigated [20]. The second one is to increase the material permittivity of the substrate where the metallic patterns are printed [21]. This method is applicable to nearly all the metamaterial structures as long as high dielectric materials can be found. Using high permeability material has a similar effect on the electrical size reduction. The third method is geometry design, where we revisit the geometry of the ring thoroughly in order to give an optimized geometry having a smaller electrical size. For example, the SRR proposed in [22] is optimized by utilizing face coupled capacitance as opposed to edge coupled capacitance in the conventional SRR designs [7], permitting a smaller electrical size in addition to the removal of the bianisotropic effect. The geometry design has not been investigated in detail but has potential improvement on the metamaterial design with small electrical size. In this paper, we applied the geometry design method, and experimentally realized a left-handed metamaterial with Crankled S-ring Resonators (CSR). When keeping all other parameters, such as the dielectric constant of the substrate and the gap between the two rings to be the same, the electrical size of the CSR is 2.5 times smaller

than the original S-ring Resonator (SR), which shows the effectiveness of the geometrical design method to achieve homogenous left-handed metamaterials. The other two methods can still be used after the geometry of the ring is optimized, allowing an enhanced ratio of the wavelength to the structure size.

2. GEOMETRY DESIGN TO REALIZE CRANKLED S-RING RESONATOR

The CSR is shown in Fig. 1(b), with the SR shown in Fig. 1(a) as a comparison. The wave is incident along the $\hat{x}$ direction with a $\hat{z}$ polarization (E_z). Under a magnetic induction H_y, the equivalent circuit model [15] for these two resonators is shown in Fig. 1(c), where C is the effective capacitance between the top and bottom metallic strips, C_1 is the effective capacitance between the central metallic strips and L is the effective inductance proportional to the area enclosed by the two half rings. With the same dimensions of the two structures, we see that the C_1 of CSR in Fig. 1(b) is larger than that of SR in Fig. 1(a). So the resonant frequency of the CSR is expected to be smaller than that of the SR. In order to further reduce the resonant frequency, the top and bottom horizontal strip in the two reversed crankled S-shaped metallic patterns are shorted at the indicated positions by metallic vias. Therefore, only the equivalent capacitance C_1 is left and the total capacitance around the loop is increased.

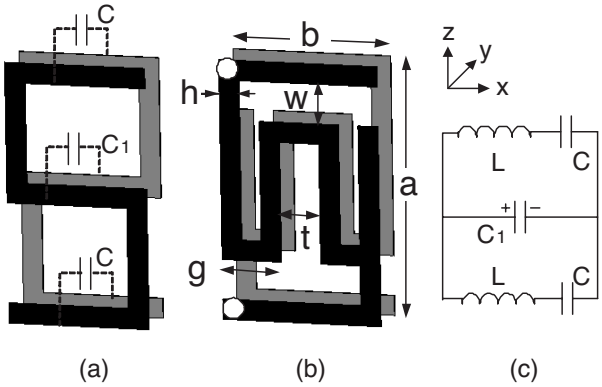

Figure 1. (a) S-ring resonator. (b) The crankled S-ring resonator. The effective capacitance C_1 is enlarged by crankling the central metallic strips. The while circles in the top and bottom horizontal strips indicate the positions of the vias. (c) The equivalent circuit for the two rings.

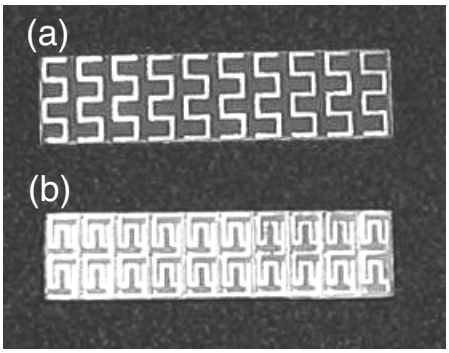

Figure 2. The slice of the two metamaterial sample: (a) the S-ring resonator, and (b) the crankled S-ring resonator.

The transmission experiment is carried out to determine the left-handed pass band of the CSR material. In the experiment, the metallic patterns are printed on the substrate with a relative permittivity of $\epsilon_r = 4$ and a thickness of $d = 1\,\text{mm}$. Fig. 2(a) shows the slices of the CSR samples, where each unit of the sample composed of two rings connected head to tail in the $\hat{z}$ direction. The dimensions of the CSR are: $a = 5.2\,\text{mm}$, $b = 3.2\,\text{mm}$, $h = 0.4\,\text{mm}$, $g = 1.2\,\text{mm}$, $t = 0.8\,\text{mm}$, and $w = 0.8\,\text{mm}$. In each unit cell there are vias through the substrate to short the front and back horizontal strips. The periodicity of the two structures along the $\hat{x}$ direction is 4 mm and the slice is repeated in the $\hat{y}$ direction in air with a periodicity of 2 mm. Along the incident direction there are 10 unit cells. The sample is placed in a parallel waveguide and the transmission results are shown in Fig. 3(a), where it can been seen that there are mainly three pass bands: $4.8 \sim 5.6\,\text{GHz}$, $7.3 \sim 9.1\,\text{GHz}$, and $10.1 \sim 11.5\,\text{GHz}$. Numerical simulations also show similar result, except for some small shift in the pass band position, as shown in Fig. 3(b).

Two methods are used to identify the left-handed pass band. The first one is using a constitutive parameters retrieval method [24]. A plane wave with E_z polarization is modeled and normally incident onto the slab of the sample along the $\hat{x}$ direction. The sample here is composed of one unit cell along the propagation direction. The scattering parameters are obtained, based on which the effective permittivity and permeability of the sample is calculated, as shown in Fig. 4. We see that in the pass band from 4.8 to 5.6 GHz, the real part of the permittivity and permeability are simultaneously negative, indicating a left-handed pass band, while in the other two pass bands both the permittivity and permeability are positive, indicating right-

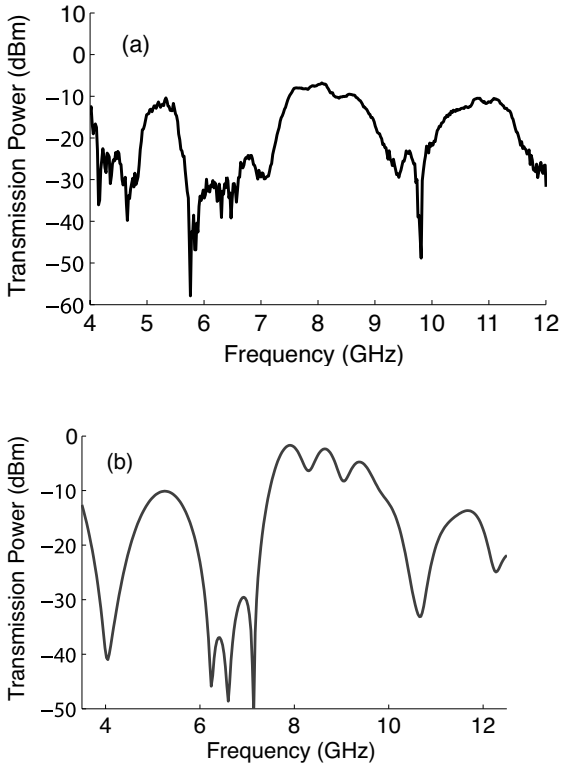

Figure 3. Transmission results for the CSR (a) experiment measurement, (b) numerical simulation.

handed pass bands.

The second method we used is the phase tracking measurement [12]. We simulate a continuous plane wave with a frequency of 5 GHz incident from left side onto the slab of the metamamterial. Fig. 5 depicts the electric field distribution within one period in a 6 cells slab. It is clearly visible that inside the metamaterial sample, the wave fronts propagate toward the source, indicating a backward wave propagation. From the result, we further confirm that the frequency band of $4.8 \sim 5.6$ GHz is a left-handed pass band.

The structural size of CSR is about $\lambda/15$. We compare it with the original SR with the same periodicity [15]. The left-handed pass band of the original S-ring occurs from 10.9 GHz to 13.5 GHz, corresponding to a structural size of about $\lambda/6$ [15]. We see that the electrical size of the CSR (only 1/2.5 of that of SR) is greatly reduced by the pattern

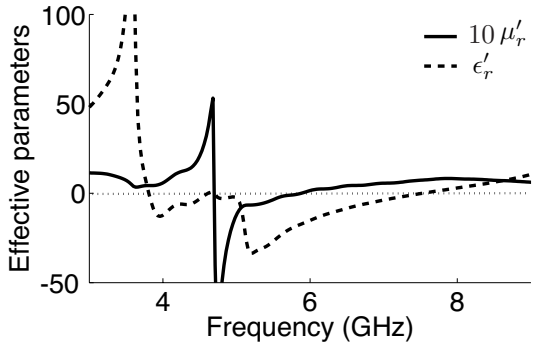

Figure 4. Real part of the permittivity and permeability of the CSR.

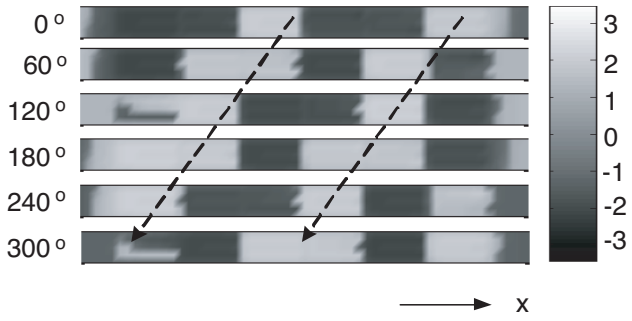

Figure 5. Electrical field distribution inside the slab of metamaterial when it reaches steady state. The continuous plane wave at 5 GHz is incident from left. There are six unit cells along the $\hat{x}$ direction. The arrows with dashed line indicate the phase front propagates along the $-\hat{x}$ direction.

optimization. In additional to the merit of small structure size, the CSR still keeps the same advantages of the SR, such as: a stand alone structure without the need of the additional rods, a simple geometry pattern that is easy to fabricate, and stable performance, etc.

3. OTHER METHODS TO REDUCE THE ELECTRICAL SIZE OF METAMATERIAL

Besides the method of geometry design, there are two other methods that can be used to further reduce the electrical size, such as: substrate optimization, parameters optimization etc. The reason of

using substrate parameters to reduce the metamaterial size is that as the permittivity and permeability of the substrate increases, the effective capacitance and inductance in the loop increases, and the resonant wavelength of the structure also increases. We fabricate two SR metamaterials with different substrates as a demonstration. In Fig. 6(a), the SR is printed on the FR4 substrate with permittivity of $\epsilon_r = 4$ and thickness of $d = 1\,\text{mm}$, then layers of the slices are aligned alternately with layers of foam substrate with permittivity of $\epsilon_r = 1$ and thickness of 1 mm. We call it S-ring with FR4+foam substrate. In Fig. 6(b), the difference of the structure from the former one is that layers of the slice with the printed S-shaped geometry are aligned alternately with layers of empty FR4 substrate with thickness of 1 mm. We call it S-ring with FR4+FR4 substrate. The transmission experimental results for the two samples are shown in Fig. 6(c), where

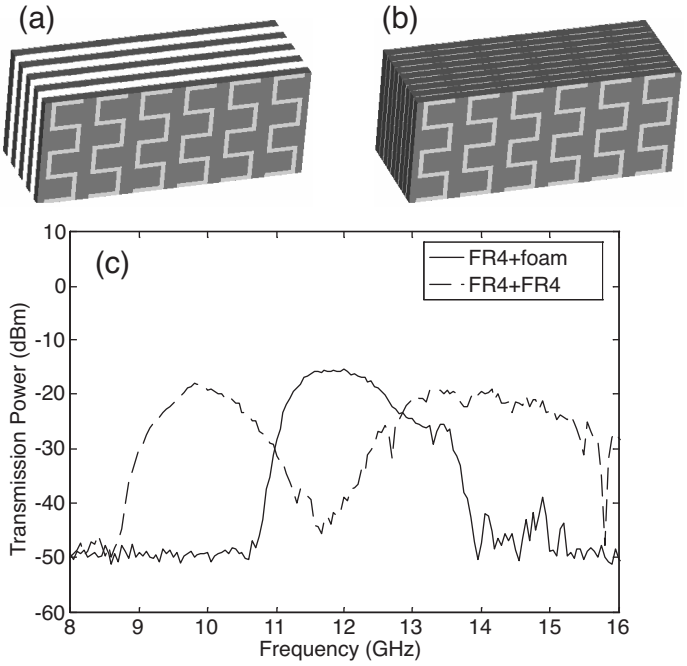

Figure 6. (a) SR with FR4+foam structure: layered of the FR4 substrate (dark color) printed with S-shaped resonator are aligned with layered of foam slice (white color). (b) SR with FR4+FR4 structure: layered of the FR4 substrate printed with SR are aligned with layered of empty FR4 substrate. (c) Transmission results for the two metamaterials.

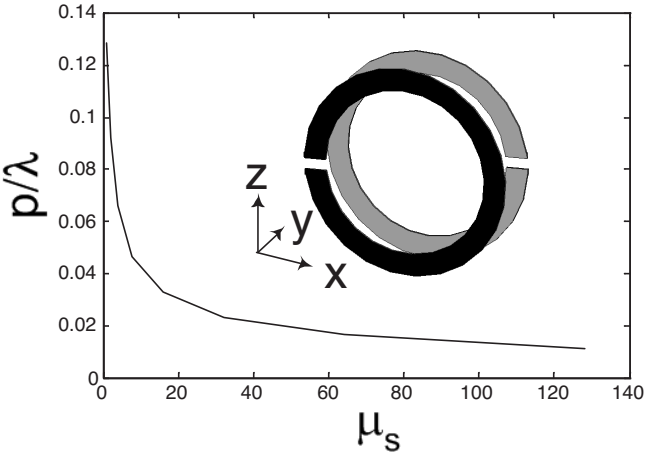

Figure 7. Simulated result on the structure size of the broad-side coupled SRR as a function of the permeability of the substrate. The inner radius of the SRR is $r = 1.6$ mm, the width of the metal strip is $d = 0.4$ mm, and the thickness of the substrate is $g = 0.4$ mm. the period of the structure is 6 mm, 1.2 mm and 6 mm in the $\hat{x}$, $\hat{y}$, and $\hat{z}$ directions, respectively.

for the FR4+foam sample, the left-handed pass band is from 10.9 to 13.5 GHz, while for the FR4+FR4 sample, the left-handed pass band is from 8.9 to 11.2 GHz. We can see the structural size is reduced by 1.2 through this method. The improvement is not very significant because we only increase the permittivity in every other layer of the substrate in the S-ring (from FR4+foam structure to FR4+FR4 substrate). If we increase the permittivity of each layer of the substrate, the improvement can be more significant (for example, compare FR4+FR4 structure with foam+foam structure). The structural size is usually proportional to $1/\sqrt{\epsilon}$ [23]. Note that it is not necessary to increase the permittivity of the whole background material. The effective capacitance of the structure is only proportional to the permittivity of the substrate that located between the metallic strips, only increasing the permittivity in these parts is enough to decrease the structural size of the metamaterial. The disadvantage of the method is that high dielectric materials are expensive to get, especially in the high frequency regime.

Increasing the permeability of the substrate also decrease the size of the structure. We use the broadside coupled split-ring resonator [22] shown in the inset of Fig. 7 as an example. The size of the ring is list in the figure caption. We simulate the resonant frequency of the SRR

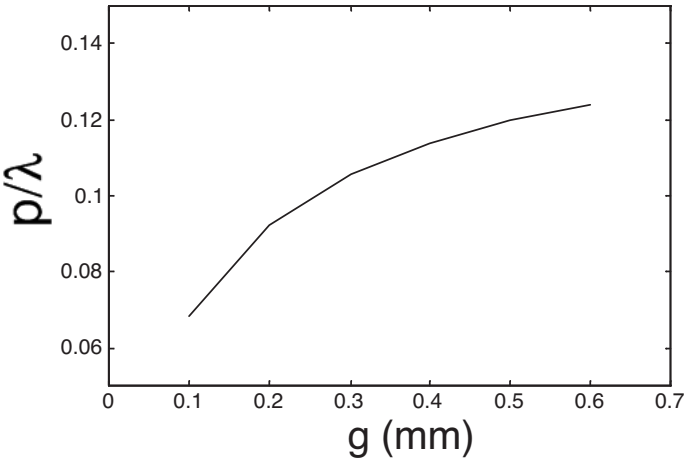

Figure 8. The structural size of the broad-side coupled SRR as a function of the gap distance.

with different values of the permeability of substrate μ_s. The structure size described by the resonant wavelength (p/λ) as a function of the permeability of the substrate μ_s is presented in Fig. 7. We see that if $\mu_s > 50$, the electrical size is decreased to be $\lambda/50$. However, it is hard to implement this method in practice because magnetic materials with $\mu_s > 50$ at microwave frequency cannot be found so far.

If the metallic patterns and the substrate parameters are fixed, we can optimize the size of the structure to further decrease the electrical size. From the equivalent circuit model [23], the resonant frequency is determined by $\omega = 1/\sqrt{LC}$, where L and C are the total effective inductance and capacitance respectively. If the resonant frequency is reduced, the electrical size of the structure is decreased compared to the working wavelength. The effective inductance is proportional to the area encircled by the loop, while the effective capacitance is determined by the overlapping area of the two half metallic loops. Here, we still use the SRR structure shown in Fig. 7 as an example. What we can optimize are the radius r, the width of the metallic strips d, and the gap between the two half metallic loops g. An increase of r increases the total area encircled by the metallic rings, so L will increase, however, since the periodicity in the xz plane is fixed, the maximum of the r is also fixed, the electrical size of the ring will reach a critical value. Therefore, optimizing the radius of the ring is not very efficient. Increase the width d lead to an increase of the capacitance but a decrease of the effective area encircled by the ring, thus a decrease

of the inductance. There will be some optimized parameters that the electrical size can be optimized to be the minimum, but still, is not very efficient. The decreasing of the g lead to an increase of the C, while the inductance still keep the same, the electrical size of the structure can be greatly decreased. With other parameters of the SRR unchanged, we make a simulation on the structure and get the resonant frequency corresponding to different g. The structure size as a function of g is shown in Fig. 8, where we see the size is greatly reduced as g decreases. Note that decreasing g is more effective than optimizing other parameters since the minimum of the g that can be achieved in experiment is only depend on the technical level of the realization.

4. CONCLUSION

In conclusion, we have proposed a crankled S-shaped ring resonator with small electrical size by using geometry optimization. The size is reduced by 2.5 times smaller than the previous reported S-ring resonator. In addition, we summarize two other methods, the substrate optimization and structure parameters optimization, which can be used to reduce the structure size of the metamaterial. Both the merits and defects of these optimization methods are discussed, and the physics insight using these method to reduce the structure size are pointed out from an equivalent circuit viewpoint. The methods proposed here offer an important flexibility to homogenize the left-handed metamaterials, which is very important in the applications of the metamaterials.

ACKNOWLEDGMENT

This work was supported in part by the Chinese Natural Science Foundation under Grant No. 60531020, 60371010, and 60671003, in part by the China Postdoctoral Science Foundation under Grant No. 20060390331, in part by ZJNSF R105253, in part by the Office of Naval Research under Contract N00014–01–1–0713, and in part by the Department of the Air Force under Air Force Contract F19628–00–C–0002.

REFERENCES

1. Veselago, V. G., "The electrodynamics of substances with simultaneously negative values of ϵ and μ," *Sov. Phys. Usp.*, Vol. 10, No. 4, 509, 1968.
2. Ran, L., J. Huangfu, H. Chen, X. M. Zhang, K. Chen, T. M. Grzegorczyk, and J. A. Kong, "Experimental study on

several left-handed matamaterials," *Progress In Electromagnetics Research*, PIER 51, 249, 2005.

3. Sui, Q., C. Li, L. L. Li, and F. Li, "Experimental study of lambda/4 monopole antennas in a left-handed meta-material," *Progress In Electromagnetics Research*, PIER 51, 281–293, 2005.
4. Pendry, J. B., A. J. Holden, D. J. Robbins, and W. J. Stewart, "Magnetism from conductors and enhanced nonlinear phenomena," *IEEE Trans. Microw. Theory. Tech.*, Vol. 47, No. 11, 2075, 1999.
5. Pendry, J. B., A. J. Holden, D. J. Robbins, and W. J. Stewart, "Low frequency plasmons in thin-wire structures," *J. Phys. C.*, Vol. 10, 4785, 1998.
6. Wu, B.-I., W. Wang, J. Pacheco, X. Chen, T. M. Grzegorczyk, and J. A. Kong, "A study of using metamaterials as antenna substrate to enhance gain," *Progress In Electromagnetics Research*, PIER 51, 295–328, 2005.
7. Shelby, R. A., D. R. Smith, and S. Schultz, "Experimental verification of a negative index of refraction," *Science*, Vol. 292, No. 6, 77, 2001.
8. Grzegorczyk, T. M., X. Chen, J. Pacheco, J. Chen, B.-I. Wu, and J. A. Kong, "Reflection coefficients and Goos-Hanchen shifts in anisotropic and bianisotropic left-handed metamaterials," *Progress In Electromagnetics Research*, PIER 51, 83, 2005.
9. Maslovski, S., P. Ikonen, I. Kolmakov, S. Tretyakov, and M. Kaunisto, "Artificial magnetic materials based on the new magnetic particle: metasolenoid," *Progress In Electromagnetics Research*, PIER 54, 61, 2005.
10. Bilotti, F., A. Alu, N. Engheta, and L. Vegni, "Anomalous properties of scattering from cavities partially loaded with double-negative or single-negative metamaterials," *Progress In Electromagnetics Research*, PIER 51, 49, 2005.
11. Chew, W. C., "Some reflections on double negative materials," *Progress In Electromagnetics Research*, PIER 51, 1, 2005.
12. Grzegorczyk, T. M., C. D. Moss, J. Lu, X. Chen, J. Pacheco Jr., and J. A. Kong, "Properties of Left-Handed metamaterials: transmission, backward phase, negative refraction, and focusing," *IEEE Microwave Theory and Tech.*, Vol. 53, 2956, 2005.
13. Ran, L., J. Huangfu, Y. Li, H. Chen, X. M. Zhang, K. Chen, and J. A. Kong, "Microwave solid-state left-handed material with a broad bandwidth and an ultralow loss," *Physical Review B*, Vol. 70, 073102, 2004.

14. Chen, H., L. Ran, J. Huangfu, X. M. Zhang, K. Chen, T. M. Grzegorczyk, and J. A. Kong, "Magnetic properties of S-shaped split-ring resonators," *Progress In Electromagnetics Research*, PIER 51, 231, 2005.
15. Chen, H., L. Ran, J. Huangfu, X. M. Zhang, K. Chen, T. M. Grzegorczyk, and J. A. Kong, "Left-handed materials composed of only S-shaped resonators," *Phys. Rev. E.*, Vol. 70, 057605, 2004.
16. Luo, C., S. G. Johnson, J. D. Joannopoulos, and J. B. Pendry, "All-angle negative refraction without negative effective index," *Phys. Rev. B.*, Vol. 65, 201104, 2002.
17. Kong, J. A., *Electromagnetic Wave Theory*, EMW Publishing, 2005.
18. Yao, H. Y., L. W. Li, Q. Wu, and J. A. Kong, "Macroscopic performance analysis of metamaterials synthesized from microscopic 2-d isotropic cross split-ring resonator array," *Progress In Electromagnetics Research*, PIER 51, 197, 2005.
19. Caloz, C., A. Lai, and T. Itoh, "The challenge of homogenization in metamaterials," *New Journal of Physics*, Vol. 7, 167, 2005.
20. Aydin, K., I. Bulu, K. Guven, M. Kafesaki, C. M. Soukoulis, and E. Ozbay, "Investigation of magnetic resonances for different split-ring resonator parameters and designs," *New Journal of Physics*, Vol. 7, 168, 2005.
21. Quan, B. G., C. Li, Q. Sui, J. J. Li, W. M. Liu, F. Li, and C. Z. Gu, "Effects of substrates with different dielectric parameters on left-handed frequency of left-handed materials," *Chinese Physics Letters* , Vol. 22, No. 5, 1243, 2005.
22. Marques, R., F. Medina, and R. Rafii-El-Idrissi, "Role of bianisotropy in negative permeability and left-handed metamaterials," *Phys. Rev B.*, Vol. 65, 144440, 2002.
23. Chen, H., L. Ran, J. Huangfu, T. M. Grzegorczyk, and J. A. Kong, "Equivalent circuit model for left-handed metamaterials," *J. Appl. Phys.*, Vol. 100, 024915, 2006.
24. Chen, X., T. M. Grzegorczyk, B.-I. Wu, J. Pacheco, and J. A. Kong, "Robust method to retrieve the constitutive effective parameters of metamaterials," *Phys. Rev. E.*, Vol. 70, 016608, 2004.